Characterization of Rock Fabric and Fluid Fairway for Hydrocarbon Imprint and Lateral Prediction.

O.J. Rotimi, Ph.D.[1,2*]; Zhenli Wang, Ph.D.[2]; and B.D. Ako, Ph.D.[3]

[1]Petroleum Engineering Department, Covenant University, Ota, Nigeria.
[2]Key Laboratory of Petroleum Resources, Institute of Geology and Geophysics, CAS, Beijing, China.
[3]Applied Geophysics Department, Federal University of Technology, Akure, Nigeria.

E-mail: oluwatosin.rotimi@covenantuniversity.edu.ng*

ABSTRACT

This work made use of computed data from well logs, with migrated seismic data, to evaluate rock fabric, reservoir fluid, and lithology of an unconsolidated alluvial fan deposit. Acoustic and elastic parameters amongst other logs were computed and used to characterize the subsurface reservoir. This was done to ascertain the possibility and success of well logs derived rock physics parameters in characterizing reservoirs. With the use of soft computing methods and stochastic algorithms, the objectives of this study were achieved. Results were presented in maps and model volumes. Lambda, Mu, Rho, and SP logs were the main inputs in the characterization based on both their individual potential and an integrated convolved potential. Filtered zones identified on cross-plot were applied to simulated volumes of LambdaRho and MuRho, gave good account of its ability to discriminate rock and fluid distribution. RGB visualization tool applied to the models gave a volume that was used to condition litho-units simulation with commendable results.

(Keywords: Lambda, mu, acoustic impedance, elastic impedance, reservoir characterization, RGB, alluvial fan, density)

INTRODUCTION

The sensitivity of seismic wave velocities (compressional and shear, V_p, V_s) to critical reservoir parameters, such as porosity, lithofacies, pore fluid type, saturation, and pore pressure, has been recognized for many years (Biot, 1956; Conolly, 1999; Perez, 2010; Goodway, 2001; Levin and Markov, 2004). However, the practical need to quantify seismic-to-rock-property transforms and their uncertainties has become most critical over the past decade, with the enormous improvement in seismic acquisition and processing, and the need to interpret amplitudes for hydrocarbon detection, reservoir characterization, and reservoir monitoring. Discovering and understanding the seismic-to-reservoir relations has been the focus of rock physics research. Post-depositional changes such as diagenesis and cementation often affect the outlook of sediments which may be seen on a blanket scale on seismic data. But well control tells more due to its proximity to the studied rocks (Wold, *et al*., 2008).

Bosch *et al*. (2010), in an attempt to quantify uncertainty reviewed seismic inversion schemes (deterministic and Stochastic) that incorporate rock-physics information and geostatistical models of spatial continuity. This focused on techniques that go beyond inverting for the elastic parameters (e.g., impedances, elastic moduli) and try to infer reservoir properties of interest, such as rock fabrics, lithologies, porosity, and fluid saturations. The transformation of any geophysical data into physical properties of the earth such as elastic or electrical parameters can be posed as an inverse problem. General inverse theory is a mathematically rich discipline, and many excellent books on geophysical inverse theory now exist (Fjaer *et al.,* 2008; Mavko *et al.,* 2003; Avseth *et al.,* 2005 etc). However, transforming seismic data to reservoir properties is an inverse problem with a non-unique solution.

Even for noise-free data, the limited frequency of recorded seismic waves makes the solution non-unique. A robust review will be that which will focus on methods of conventional subsurface mapping for reservoir characterization that features geology, rock-physics and/or petrophysical knowledge incorporating seismic inversion and geostatistics (Figure 1). A

combination of elastic-property estimates from seismic inversion and rock physics or petrophysics for predicting reservoir properties is a key and classical procedure in reservoir characterization (Biondi *et al.,* 1998). However, the requirement for a scale dependent variogram and weight allocations has to some degree been overlooked in geostatistical simulation (which has moved to the realm of multivariate applications to handle probabilistic assignments on a direct or transposed scale). The importance of this is in distributing rock/object properties on spatial scales within an area of interest. This constitutes a major pivotal point from which adequate comparison and prediction can stem off because the traditional variogram has no capacity to capture subsurface heterogeneity (Caers, 2000, 2002). This work is aimed at adopting well logs computed rock physics and rock impedance functions (i.e. acoustic and elastic) parameter in modelling rock properties for hydrocarbon exploration.

Prediction Beyond Well Control

The cost of hydrocarbon exploration and production coupled with the attendant risk will ordinarily not allow wells to be sited at all locations on a concession. Therefore, methods of knowing the right location to explore and site wells are employed as much as possible to assist in making decision for locating a well. This vital deduction serves as consequent information sought from the initial results of this study. The possibility of successfully predicting properties away from well control prior to drilling is both a function of the terrain of investigation and available data for geostatistical predictions.

The first point about terrain refers to the ease at which plausible geo-model of the area (zone) of interest can be built such that all elements that pertains to lithological units, structural elements and basin architecture will be inculcated and well represented (Rotimi, *et al.,* 2014). The importance of this is for proper location of properties of interest at their correct elevations and positions at the subsurface for accurate production decision to be made. The substance of terrain of investigation actually rests on the shoulders of the second point which is the availability of good data points to carry out an integrated interpretation and prediction.

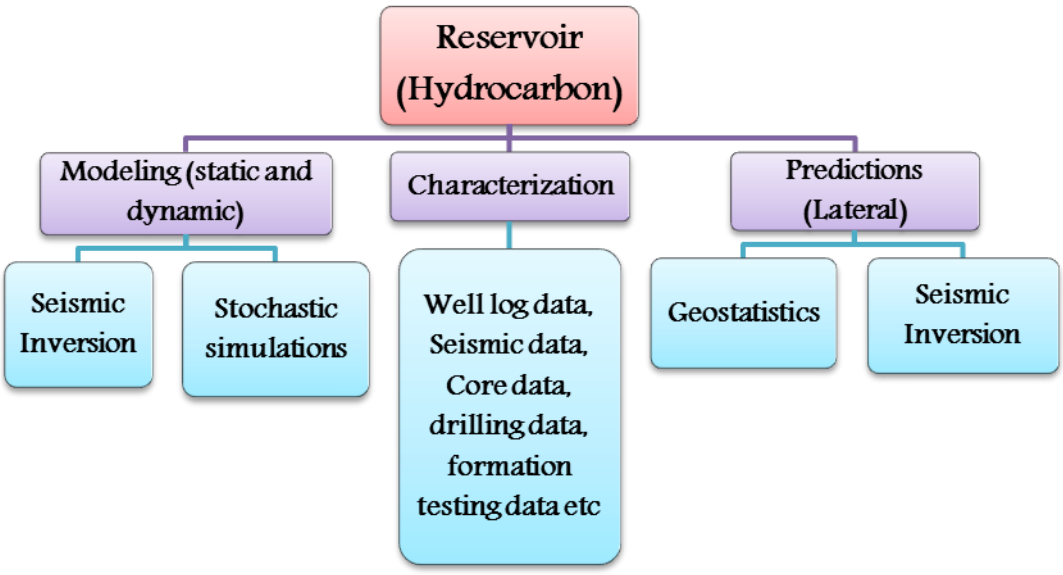

Figure 1: A Summary of Methods in Hydrocarbon Reservoir Characterization.

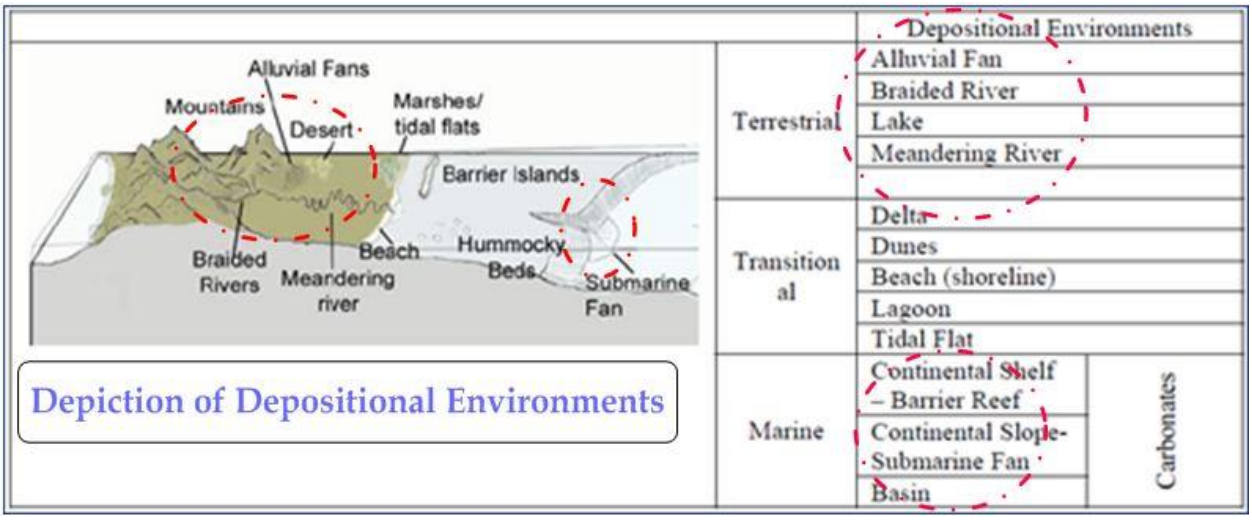

Figure 2: Depiction of Depositional Environment Showing Fan Environments (Alluvial and Submarine).

GEOLOGY OF THE STUDY AREA

Allen *et al.,* (1997) gave a good account of the episodes that saw to the emplacement of both Stratigraphic and Structural patterns of the Alluvial fan deposit in the area. Alluvial fan is an unconsolidated deposit of sedimentary rock that accumulates at the entry of an elevated landform usually a mountain or a submarine canyon (in this case a submarine fan sand is deposited). The Reason for this deposit is availability of accommodation (space for deposition). Due to lack of space or energy for transportation the content of river is dropped (Rotimi, 2010; Rotimi, *et al.,* 2014). Eustatic sea level fluctuations may also favor this.

Another reason is a pause of cessation in sediment supply from the transporting or supply water course. A 3D view of the deposit (Figure 2) shows a fan shaped structure that are often larger and more prominent in dry terrain, hence generally referred to as a desert landform. Due to their remarkable sedimentary configuration, they have high porosity resulting from rapid deposition and unconsolidation. They are renowned to host fluids and are targets for explorations programs. They serve as outlet for mountainous drainage system, therefore transfer of sediment is often accompanied by intermittent flash floods that sometimes ends in mud flows as peak deposits.

A typical cross-section of this erosional depositional system shows a Bouma channel system deposit. This is often characterized by finning upward deposits i.e. coarse sediments are laid down first and finer ones thereafter as a result of turbidity current effect. Distributaries formed carries finer sediments to deposit at flanks and apex as the energy wanes. Infiltration also occurs during the process of channel cutting. Downward percolation makes fluids settle in porous and permeable layers and preserved as reservoirs that are explored.

METHODOLOGY

Well logs used were corrected for environmental effect with Schlumberger standard charts. They were normalized before being used for computations. Rock physics parameters of acoustic and elastic moduli (AI, EI, Lambda, Mu, P-vel, S-vel, Vp/Vs, Poisson ratio) were of interest and carefully computed with equations (1 – 11) presented in the next section. These logs correlated with results of core analysis on the cored well G19 (Figure 3) as indicated in Table 1.

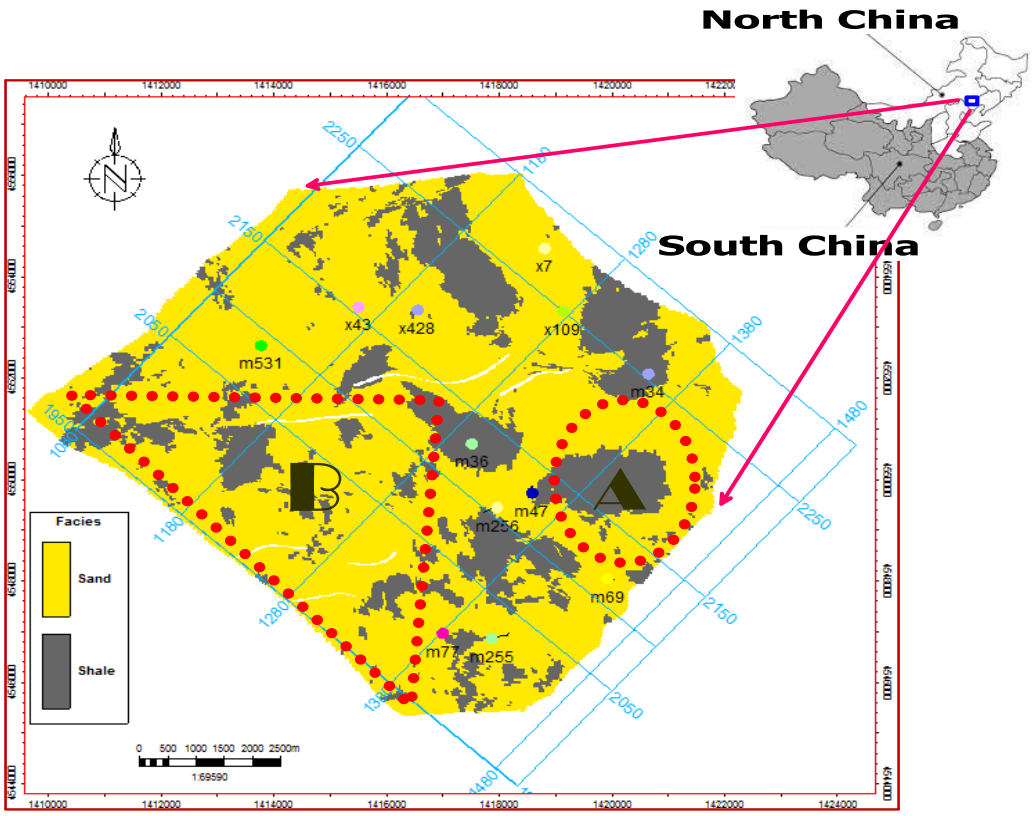

Figure 3: Study Area Showing Object Captured Locations Outside Well Control.

Table 1: Types and Descriptions of Well Logs.

Description	Lithology	Resistivity (Saturation)	Porosity/ Petrophysical	Predicted	Computed
Well logs (for some other wells)	Spontaneous Potential (SP)	Deep Laterolog (LLD)	Sonic/ Acoustic	Density, Neutron, Facies	Volume of shale (V_{sh}), Bulk Volume water (BVW) Porosity (ϕ), Water Resistivity (R_w), Water Saturation (S_w), Hydrocarbon Saturation (S_{hc}), Permeability (K), P-Velocity (V_p), S-Velocity (V_s), Poisson ratio, Lambda, Mu, Density (ρ), V_p/V_s ratio, Acoustic Impedance (AI), Elastic Impedance (EI10,20,30)
G19 (well with core data)	Spontaneous Potential (SP), Gamma Ray (GR)	LLD	Bulk density, Neutron, Core Permeability		

Formulae for the Logs Rock Properties used in Logs Computing

$$EI = V_p^{(1+Sin^2\theta)} V_s^{(-8\times K Sin^2\theta)} \rho_b^{(1-4\times K\times Sin^2\theta)} \quad (1)$$

Elastic impedance equation from Conolly, (1999), Batzle and Wang, (1992),

Where V_p is compressional velocity, V_s is shear velocity, K is constant representing the average V_s^2/V_p^2 for interval, P_b is bulk density and Θ is incidence angle (10, 20, and 30).

$$V_{s(km/s)} = a.V_p^2 + b.V_p + c \quad (2)$$

AC shear equation computed using the curve mineral method. V_{sh} curve used and other curves becomes 1-V_{sh}.

Where a is 0, b is 0.76969 and c is 0.86735.

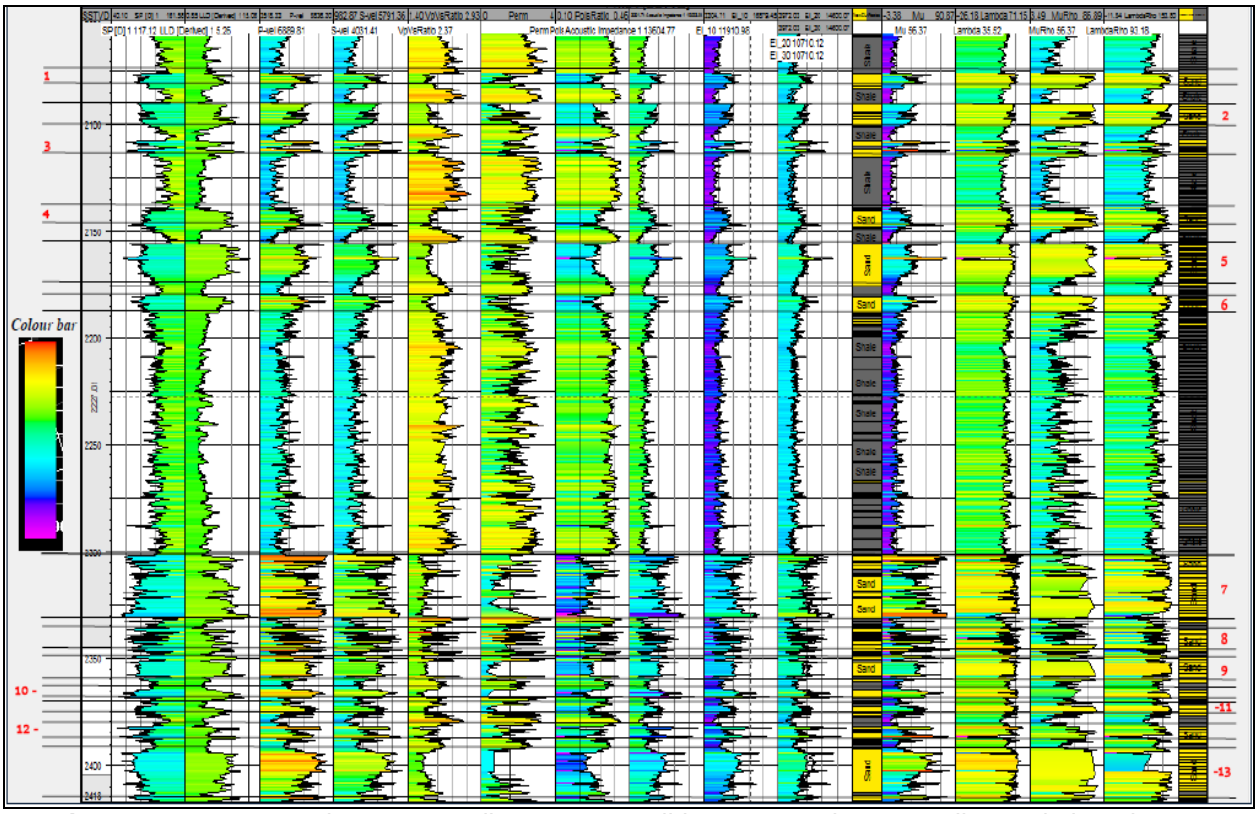

Figure 4: 16 Computed Logs on Well G19. 13 Candidate Reservoir Tops Delineated also Shown.

$$V_s = \frac{1}{2}\left\{\left(\sum_{i-1}^{4} X_i \times VS_i\right) + \left(\sum_{i-1}^{4} X_i / VS_i\right)^{-1}\right\} \quad (3)$$

The Voigt-Reuss-Hill averaging technique for V_s Where X_i is volume of *i*th mineral, VS_i is shear velocity of *i*th mineral and VS is shear velocity.

$$v = \frac{V_p^2 - 2V_s^2}{2\left(V_p^2 - V_s^2\right)} \quad (4)$$

Poisson Ratio Equation (v)

Where V_p is compressional velocity and V_s is shear velocity.

$$Mu = \mu = \rho V_s^2 \quad (5)$$

$$Lambda = \lambda = \rho V_p^2 - 2\rho V_s^2 \quad (6)$$

$$V_p = \sqrt{\frac{\lambda + 2\mu}{\rho}} \quad (7)$$

$$V_s = \sqrt{\frac{\mu}{\rho}} \quad (8)$$

Therefore:

$$Z_s^2 = (\rho V_s)^2 = \mu\rho \quad (9)$$

and,

$$Z_p^2 = \left(\rho V_p\right)^2 = (\lambda + 2\mu)\,\rho \quad (10)$$

so,

$$\lambda\rho = Z_p^2 - 2Z_s^2 \quad (11)$$

where Z_p^2 is P impedance and Z_s^2 is S impedance.

Figure 4 is a plot panel for well G19 showing all predicted and computed log curves gotten from Equations 1 – 11 and others.

All these logs are presented in 16 tracks. Their names by tracks are SP, LLD, P-vel (V_p), S-vel (V_s), V_p/V_s ratio, Permeability (K), Acoustic impedance (AI), Elastic impedance (EI 10, 20, 30), Electrofacies, Mu, Lambda, MuRho, LambdaRho, Simulated facies log. Delineated potential reservoir formations are also shown.

Static Modeling

Tracking of dominant bright reflection events on 3D Seismic data was done as an initial conventional step to building a horizon over the surface of interest. This was critically examined by attributes computation and seismic facies variations (Barnes, 2001; Rotimi, 2014). Horizons build for tops above and below zones of interest serve as delimiters for simulation casing. Computed well logs were sampled (upscaled) into this structural grid frame work as a step that precedes stochastic simulations.

RESULTS AND DISCUSSION

The classical Kriging algorithm was used to build maps of surfaces for the properties of interest. This was done after data transforms. Results of map (isomap) surfaces built from simulated properties are presented in Figure 5 a-d. Porosity value ranges between 0.1 and 0.27. The western portion of the oil field is the most porous and has wells situated strategically. The low relief of the area makes the mid portion more planar than adjacent areas. Permeability is highest at 2.4mD.

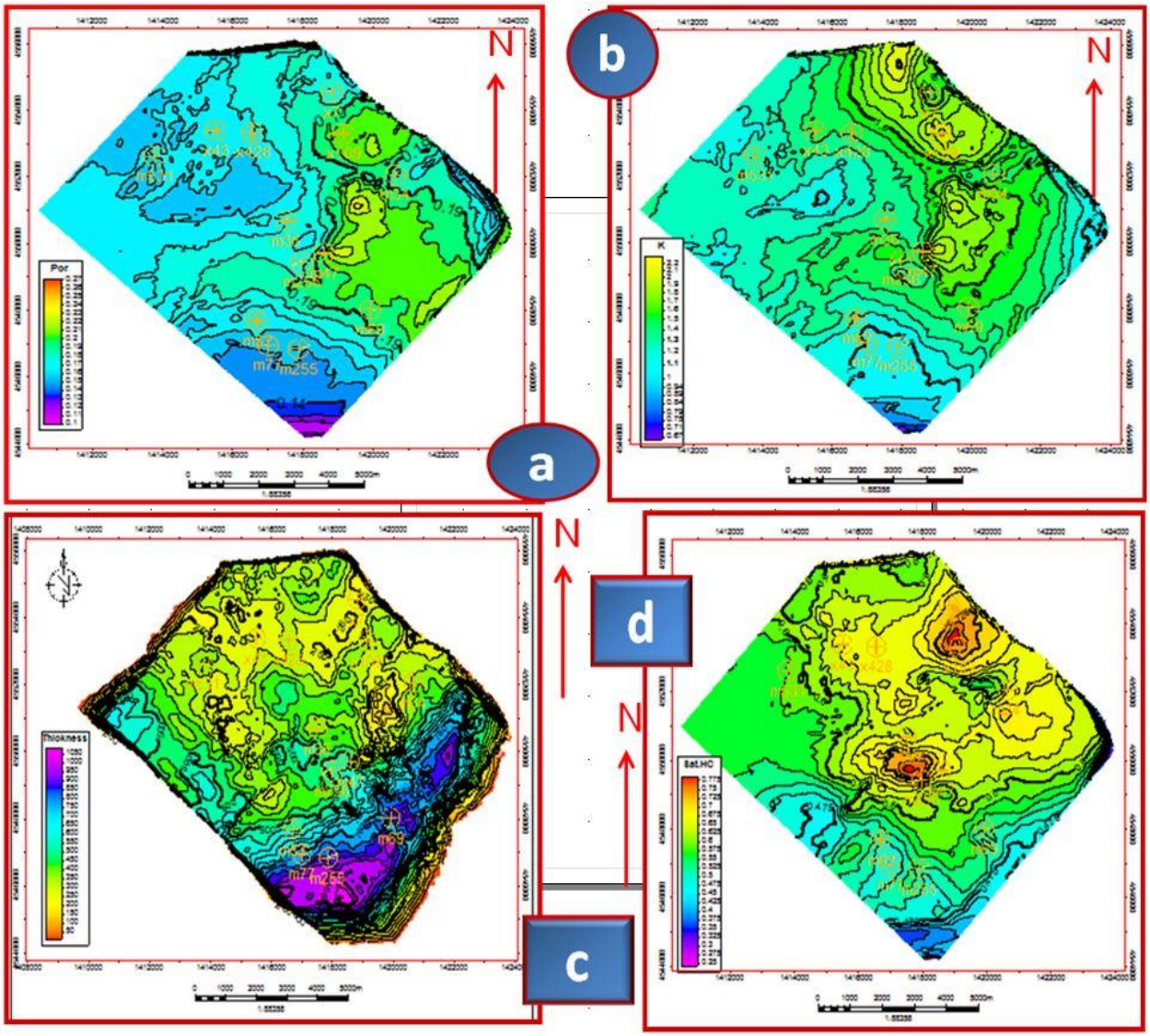

Figure 5: Average Isomaps (A-Porosity, B-Permeability, C-Isopach, D-Hydrocarbon Saturation).

The field has fairly permeable sand units with the northwest – northeast flank having the lowest permeability values. The area shown in Figure 5c is the field wide extent. However, the area of interest has a maximum thickness of 402 meters with the southern part having the most sand. Hydrocarbon saturation as seen on Figure 5d ranges from 25% - 67%. From the middle portion with the highest hydrocarbon saturation the saturation height is approximately 125 meters while slightly to the north is about 148 meters (Figure 5d).

Convolving Physical, Acoustic and Elastic Properties

The oil field explored has lithological complexities typical of the depositional environment. An approach to understand subsurface lithological distribution was to make cross-plots of properties computed and earlier analyzed. Property filters were made out of the cross-plots and subsequently applied to simulated properties.

These worked as discriminants and assisted in delineating portions with different configurations such as lithology type, rock fabrics and reservoir fluids (water and oil). Spontaneous potential (SP) logs used for the study is good for lithology identification as it records potential difference of conductive and non-conductive zones which are invariably reservoir and non-reservoir units. 4 litho-units identified by the 4 zones are sand, shale, sandy-shale and silt (Figure 6). Density (Rho) is an indicator of porosity and by implication saturation and permeability of a rock unit which are indispensable. Lambda and Mu are elastic moduli parameters that relates intrinsic properties of rocks and fluids to its elastic properties and velocity variations (Mandler and Stevens, 2004; Rao and Biswal, 2004; Hoffe, *et al.,* 2008). The product of elastic properties (Lambda and Mu) and Rho serves as discriminants to isolating rock and fluid properties. Lambda-Rho is a sensitive indicator of reservoir fluids while Mu-Rho helps to identify pure rock fabric (essentially lithology indicator) (Brown and Korringa, 1975). Figures 7 and 8 are results of filtered area of interest volumes using the various zones identified and isolated in figure 6. A bird's eye view of the cross plot result is presented in Table 2.

Table 2: Parameters from Crossplot Sample Presented in Figure 6.

Zone Parameters	MuRho	LambdaRho	Lithology/Rock Fabric	SP value
1	3 – 20	45 – 85	Shale	140 – 160
2	24 – 70	110 – 143	Sand	50 – 75
3	16 – 80	85 – 135	Sandy Shale	90 – 140
4	32 – 80	40 – 125	Shale	45 - 75

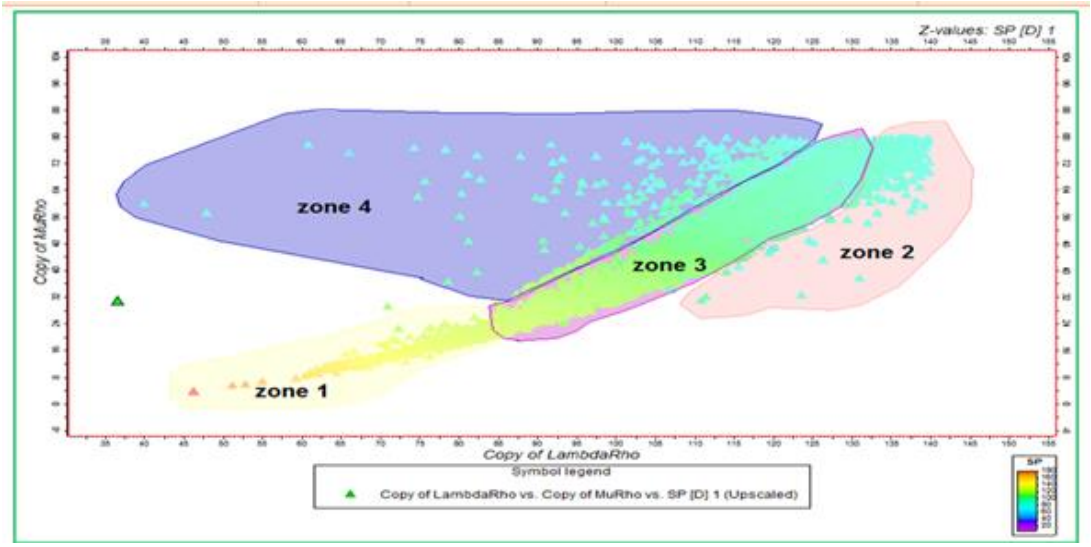

Figure 6: Four Probable Zones were Identified Viz, Zone1, Zone2, Zone3, Zone4 from Cross-Plot of LR-MR-SP.

Properties Blending

Red, Green, Blue (RGB) is a powerful visualization tool. RGB makes use of color panel variation for a visualized parameter. Conventional use of color spectrum on properties is to represent the intrinsic value of such property as realistic indices to draw judgment and make interpretations that are valid. RGB does interpolation along axis between selected or existing colors in the inputted property/parameter.

Interpolation gradient is minimized in such a way to suppress spurious effect of similar coloration from different properties. For each property in a RGB cube, two end colors are first defined, after which color mixing is done by interpolation along the axis. The success of this step can be viewed on a histogram of the input and output properties and cube. Here, the RGB cube was used to ascertain zone for correlation of values within the volume of interest.

The blend cube had MuRho, LambdaRho and SP as input. These properties introduced into the blending process resulted into a single structural geometric volume that presents textural, topographical and rock fabric features (Figure 9). A correlation line intersection showing the effect of the blending is presented in Figure 10. The continuous lighter color bands are hydrocarbon reservoir zones. This volume became a pre-profiled element used to condition and co-simulate lithology property distribution for portions beyond well location. Results shows lithological sections that agrees well with seismic reflection event patterns of this area. Hence the possibility of proffering reasonable methods of exploring the hydrocarbon in the segment.

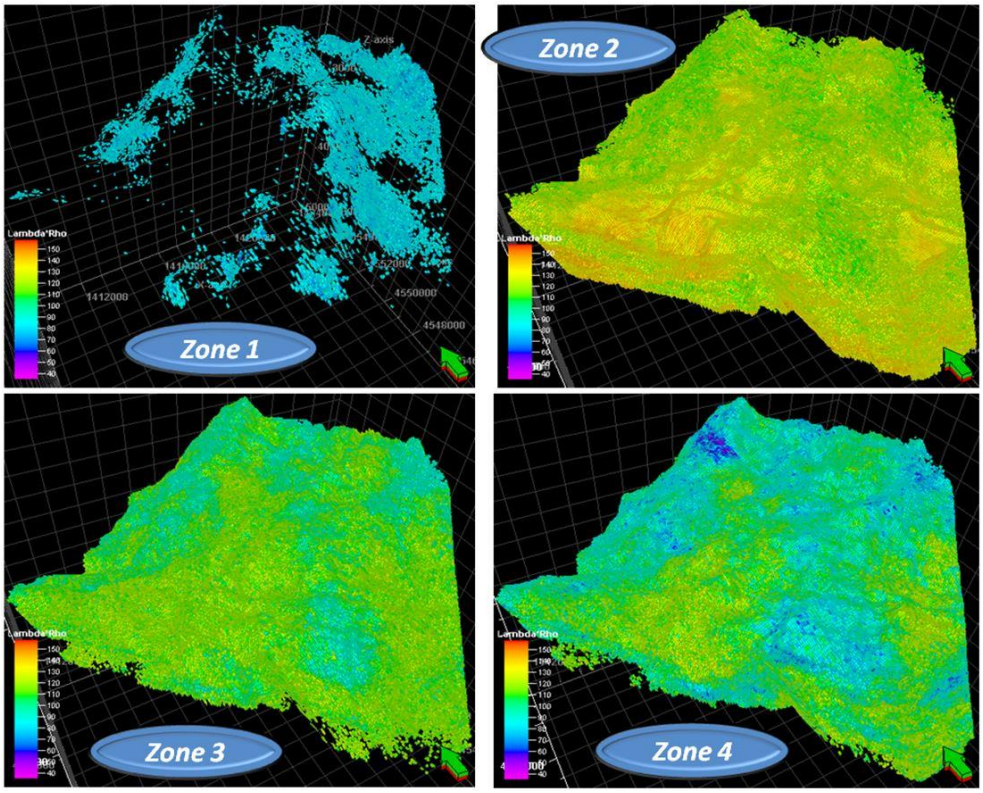

Figure 7: Lambda-Rho Volumes Subjected to Filtering from Cross-Plot Zones.

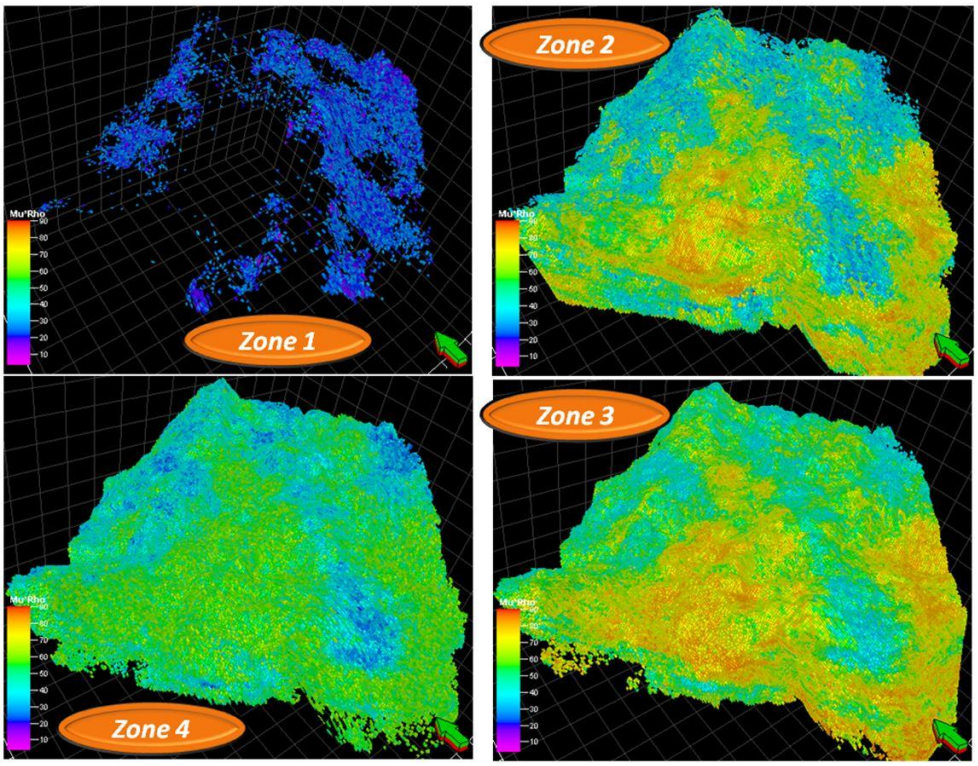

Figure 8: Mu-Rho Volumes Subjected to Filtering from Cross-Plot Zones.

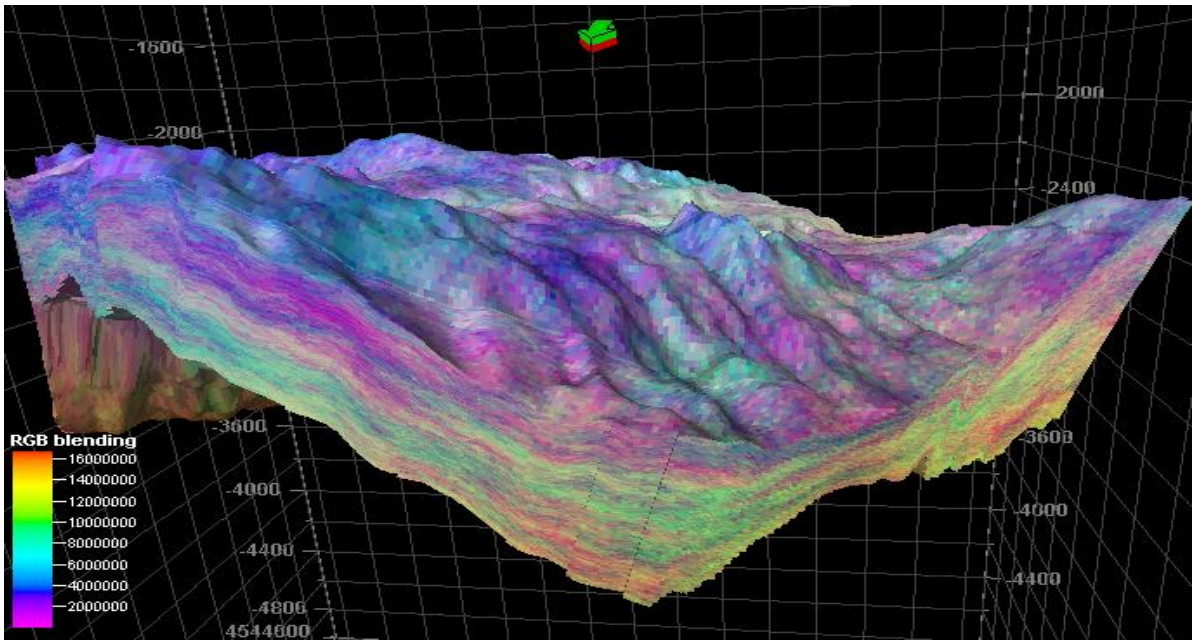

Figure 9: RGB Blending of LambdaRho, MuRho and Depth Volumes. This a Textural Lithological and Structural Geometric Visualization Tool.

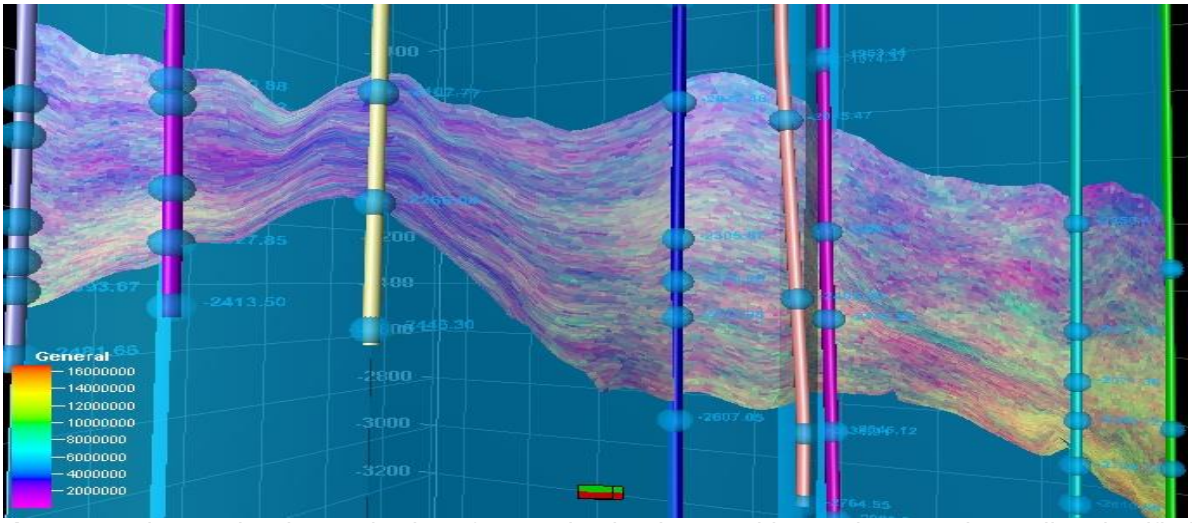

Figure 10: Line 8, Showing Projection of RGB Blend Volume. White Portions are the Earlier Identified Probable Hydrocarbon Filled Zones.

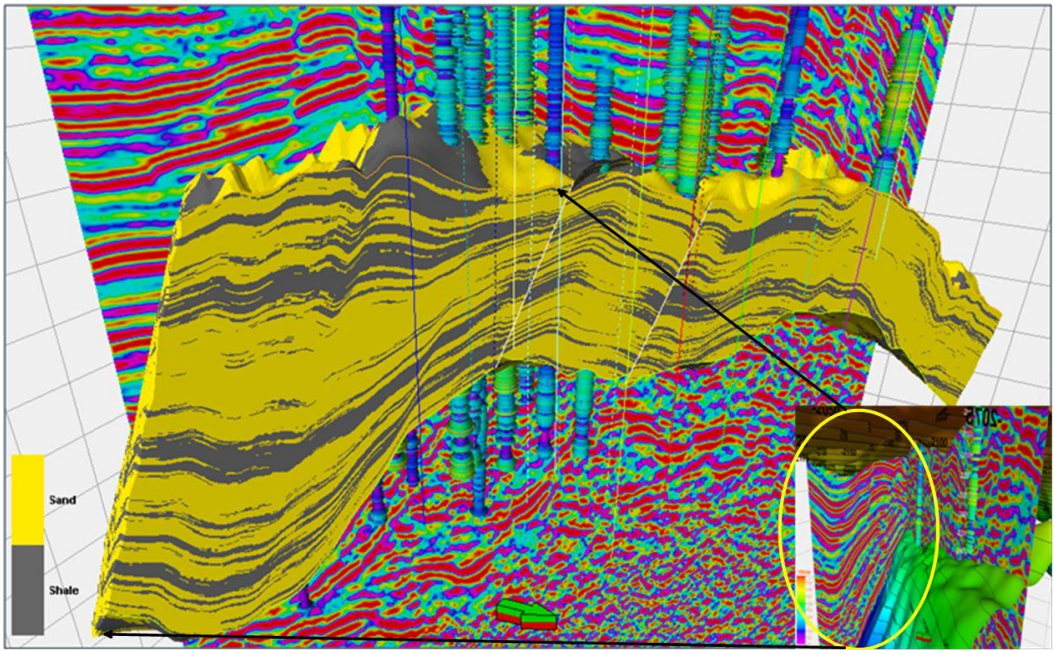

Figure 11: Intersection View of Wedge Structure from B Part of Figure 2 Showing Inline 2097 and Wells.

Lateral Predictions and Validation

Predicting rock properties beyond well control was achieved both within the wells and also outside well locations. For within well location, the model validation step adopted for this, afforded the flexibility of well point removal, model rerun and revalidation via blinding and blanketing of properties through variogram remodeling at the instance of validation. However, predicting a rock property in regions where no wells originally exists and control well is far from was a success (Figures 11-13). This is seen in the portion of the volume of interest where the thick hunk-like lithological deposits exists (Figure 11).

Figure 12-13 illustrates the stratigraphical form of the rock fabric present in this vicinity, especially in zones A and B of Figure 3. The success of this is by two reasons. Firstly, the theory of distance of the most distal well within the simulation case towards where the hunk-like structure exists was practically experimented until it was successful.

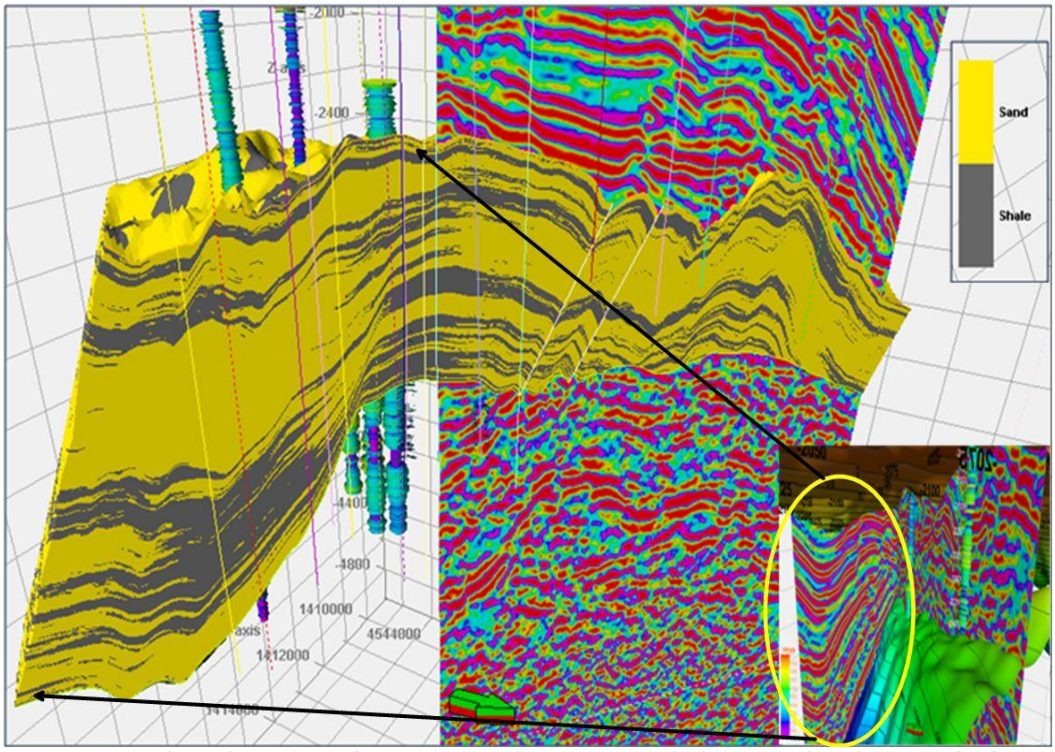

Figure 12: Intersection View of Wedge Structure from B Part of Figure 2 Showing Continuity on Inline 2097 and Wells.

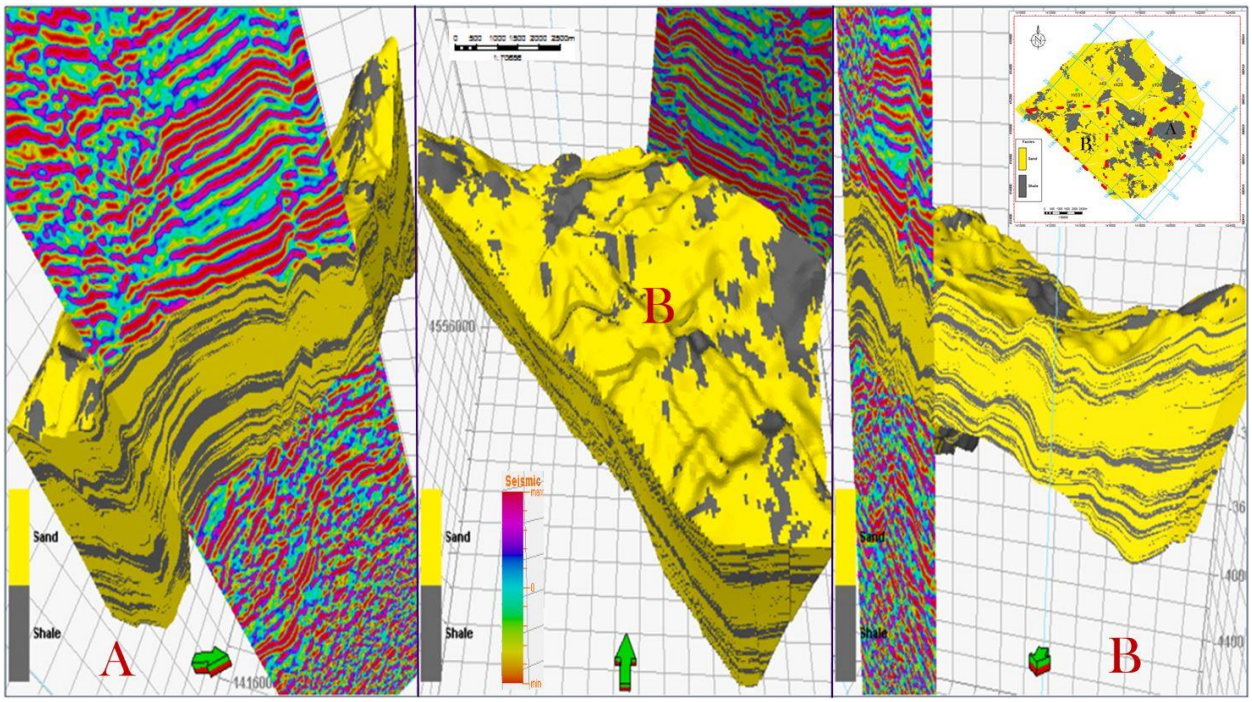

Figure 13: Intersection Block from B Figure 2 as Inset.

The second reason is for the variogram functions and algorithms utilized in the simulation processes.

The variogram elements were carefully fixed and consideration was given to data stationarity that may force ergodicity effect to set in on the simulation operation. Furthermore, in making the models, the nature of the wells were taken into account by utilizing True Stratigraphical Thickness (TST) in upscaling well logs. Thus, adequately handling scale problems and estimation bias which may set in through excessive modeling and data transformation operations.

CONCLUSION

The conventional method of obtaining acoustic and elastic rock properties has been down-played here by making use of computed well logs as against migrated seismic data for their realization. Well logs obtained from an oil field was corrected for environmental and acquisition challenges. 16 new logs were predicted and used for stochastic simulations. Spontaneous Potential (SP), Lambda, Mu and Density (Rho) logs were used for rock fabric/lithology and fluid occurrence discrimination.

Models from the volume of interest using these rock properties were filtered by zonation and captured for different facies. Sand, Shale, Sandy Shale and Silt were identified. RGB colour blending visualization assisted in projecting lateral representation of litho-units. The RGB blend volume was used to condition a new facies volume for lateral predictions beyond well location. This step was a success thereby making it possible to identify lithological configurations at more distal portions of the area of interest.

ACKNOWLEDGEMENT

The authors would like to appreciate MOST-CASTEP for the equipment donated for this research. OilChina is appreciated for the release of data used for this study. Key laboratory of Petroleum research of IGGCAS is appreciated for research collaboration and support.

REFERENCES

1. Allen, M.B., D.I.M. Macdonald, Z. Xun, S.J. Vincent, and C. Brouet-Menzies. 1997. “Early Cenozoic Two-Phase Thermal Subsidence and Inversion of the Bohai Basin, Northern China”. *Marine and Petroleum Geology*. 14(78):951-972.

2. Avseth, P., T. Mukerji, and G. Mavko. 2005. *Quantitative Seismic Interpretation*. Cambridge University Press: Cambridge, UK. 408.

3. Barnes, A.E. 2001. “Seismic Attributes in your Facies”. *CSEG Recorder*. 9:41-47.

4. Batzle, M. and Z. Wang. 1992. “Seismic Properties of Pore Fluids”. *Geophysics*. 57(11): 1396-1408.

5. Biondi, B., G. Mavko, T. Mukerji, J. Rickett, D. Lumley, C. Deutsch, R. Gundeso, and M. Thiele. 1998. “Reservoir Monitoring: A Multidisciplinary Feasibility Study”. *The Leading Edge*. 17:1404-1414.

6. Biot, M.A. 1956. “Theory of Propagation of Elastic Waves in a Fluid-Saturated Porous Solid”. *J. Acoustic. Soc. Am.* 28:168-191.

7. Bosch, M., T. Mukerji, and E.F. Gonzalez. 2010. “Seismic Inversion for Reservoir Properties Combining Statistical Rock Physics and Geostatistics: A Review”. *Geophysics*. 75(5): 75A165–75A176. DOI 10.1190/1.3478209.

8. Brown, R.J.S. and J. Korringa. 1975. “On the Dependence of the Elastic Properties of a Porous Rock on the Compressibility of the Pore Fluid”. *Geophysics*. 40(4):608-616.

9. Caers, J. 2000. “Modeling Facies Distributions from Seismic using Neural Nets”. *Stanford Center for Reservoir Forecasting Annual Report*. 1(13):1-30.

10. Caers, J. 2002. “History Matching under Training-Image based Geological Model Constraints”. *Stanford Center for Reservoir Forecasting Annual Report*. 1(15):1-19.

11. Conolly, P. 1999. “Elastic Impedance”. *The Leading Edge*. 18:438-452.

12. Fjaer, E., R.M. Holt, P. Horsrud, A.M. Raaen, and R. Risnes. 2008. “Petroleum Related Rock Mechanics”. Elsevier: Amsterdam, The Netherlands.

13. Goodway, B. 2001. “AVO and Lame’ Constants for Rock Parameterization and Fluid Detection”. *RECORDER*. 26(6):39-60.

14. Hoffe, B., M. Perez, and W. Goodway. 2008. “AVO Interpretation in LMR Space: A Primer. Expanded Abstract”. Back to Exploration - 2008 CSPG CSEG CWLS Convention. 31-34.

15. Levin, V.M. and M.G. Markov. 2004. “Elastic Properties of Inhomogeneous Transversely Isotropic Rocks”. *International Journal of Solids and Structures*. 42:393–408

16. Mandler, H. and L. Stevens. 2004. “Porosity-Thickness Prediction by Application of AVO/LMR Analysis to Seismic Data: A Case Study from a Clastic Lower Cretaceous Gas Reservoir at Crossfield, Southern Alberta”. CSEG National Convention.

17. Mavko, G., T. Mukerji, and J. Dvorkin. 2003. *The Rock Physics Handbook*. Cambridge University Press: Cambridge, UK. 340.

18. Perez, M. 2010. “Beyond Isotropy – Part II: Physical Models in LMR Space”. *CSEG RECORDER*. October: 36-42.

19. Rao, Y.H. and A.K. Biswal. 2004. “Comparative Study of AVO attributes for Reservoir Facies Discrimination and Porosity Prediction”. 5th Conference & Exposition on Petroleum Geophysics. Hyderabad, India. 498-502.

20. Rotimi, O.J. 2014. “Seismic Stratigraphic Analysis for Depositional Environment and Hydrocarbon Occurrence Appraisal”. *European Journal of Scientific Research*. 125(3):295-304.

21. Rotimi, O.J., B.D. Ako, and W. Zhenli. 2014. “Stratigraphy and Reservoir Quality of the Turbidite Deposits, Western Sag, Bohai Bay, China P.R.”. *Journal of African Earth Science*. 99(2):517-528. DOI: 10.1016/j.jafrearsci.2014.05.010.

22. Rotimi, O.J. 2010. “Sequence Stratigraphy Study within a Chronostratigraphic Framework of ‘Ningning Field’, Niger Delta”. *RMZ – Materials and Geoenvironment*. 57(4):475–500.

23. Wold, J., G.M. Grammer, and W.B. Harrison. 2008. “Sequence Stratigraphy and 3-D Reservoir Characterization of a Silurian (Niagaran) Reef – Ray Reef Field, Macomb County, Michigan”. Eastern Section AAPG, Pittsburgh, PA. 13 – 23.

SUGGESTED CITATION

Rotimi, O.J., Z. Wang, and B.D. Ako. 2015. “Characterization of Rock Fabric and Fluid Fairway for Hydrocarbon Imprint for Lateral Prediction”. *Pacific Journal of Science and Technology*. 16(1):323-335.

Pacific Journal of Science and Technology